IL-21 lowers the B cell receptor affinity threshold for participation in a T cell dependent immune response.

Alexandra R. Dvorscek[1], Craig I. McKenzie[1], Marcus J. Robinson[1], Zhoujie Ding[1], Catherine Pitt[1], Kristy O'Donnell[1], Dimitra Zotos[1], Robert Brink[2], David M. Tarlinton[1], Isaak Quast[1,3]

[1]Department of Immunology and Pathology, Monash University, 89 Commercial Rd, Melbourne 3004, Victoria, Australia.
[2]Immunology Division, Garvan Institute of Medical Research, Darlinghurst, NSW 2010, Australia; St. Vincent's Clinical School, UNSW Sydney, Sydney, NSW 2010, Australia.
[3]Corresponding Author.

Summary:

The cytokine IL-21 is a regulator of B cell responses, increasing antibody quantity and quality. Here, we report IL-21's role during germinal center initiation, where it increases the response magnitude and lowers the B cell receptor affinity threshold for participation.

Abstract:

The expansion of antigen-specific T and B cells and generation of germinal centers (GC) are prerequisites for long-lasting, high-affinity antibody-mediated immune protection. Affinity for antigen is fundamental to GC B cell recruitment as it determines access to T cell help and thus competitiveness within the response. However, how T-cell derived signals contribute to such recruitment is incompletely understood. Here we report how the signature cytokine of follicular helper T cells, IL-21, acts as a key regulator of the initial B cell response. By activating AKT and S6, IL-21 accelerates cell cycle progression and the rate of cycle entry of B cells, increasing their contribution to the ensuing GC. This effect is most pronounced on B cells receiving weak T cell co-stimulation *in vit*ro and on low-affinity B cells *in vivo*, which require IL-21 receptor signaling for their recruitment and persistence in the early response. Thus, IL-21 determines the composition of the T-dependent B cell response by regulating the breadth of BCR affinities that can participate.

Keywords:

B cells/T-dependent B cell response/Il-21/BCR affinity/Cell cycle

Introduction:

The functionality of T cell dependent (TD) B cell responses, which underlie almost all vaccine success, relies on germinal centers (GC). GC are specialized, transient structures located within follicles of secondary lymphoid organs. Here, B cells mutate the genes encoding their antigen receptor (B cell receptor, BCR) with those gaining higher affinity for antigen being selected by their interaction with T follicular helper cells (Tfh) to differentiate into antibody secreting plasma cells, long-lived memory B cells or to undergo further rounds of proliferation and BCR diversification (Mesin, Ersching et al., 2016, Zotos & Tarlinton, 2012). Within GC, Tfh-derived signals are considered to control B cell proliferation and selection (Allen, Okada et al., 2007, Gitlin, Mayer et al., 2015, Qi, Cannons et al., 2008, Zaretsky, Atrakchi et al., 2017), while during the initial phase of the response, B cell intrinsic determinants such as BCR affinity and avidity govern response participation (Kato, Abbott et al., 2020, Shih, Meffre et al., 2002). BCR ligation triggers a signaling cascade that influences B cell fate in an antigen-affinity dependent manner (Kim, Pan et al., 2006, Liu, Meckel et al., 2010) including survival, proliferation and differentiation (reviewed in (Niiro & Clark, 2002)). In addition, naïve B cells capture antigen from the surface of antigen presenting cells using pulling forces, with the BCR affinity determining the efficiency of this process and thus the access to T cell help (Schwickert, Victora et al., 2011, Spillane & Tolar, 2017). The outcome of cognate T:B interaction is then dependent on the expression of co-stimulatory molecules, adhesion molecules and the duration of the T:B interactions (Qi et al., 2008, Zaretsky et al., 2017). T cell derived cytokines such as IL-4, IL-10, IL-13 and IL-21 can also modulate human and mouse activated B cell proliferation, apoptosis and differentiation and thus potentially influence GC initiation (Ford, Sheehan et al., 1999, Good, Bryant et al., 2006, Ozaki, Spolski et al., 2004, Robinson, Pitt et al., 2019, Snapper, Finkelman et al., 1988, Tangye, Avery et al., 2003, Wagner, Hanna et al., 2000). One of these cytokines, IL-21, is produced by follicular T cells shortly after the initiation of a TD B cell response then gradually increases in amount until GC reach maturity (Chtanova, Tangye et al., 2004, Gonzalez, Cote et al., 2018, Luthje, Kallies et al., 2012, Zhang, Tech et al., 2018). The outcome of IL-21 signaling in B cells *in vitro* are multiple and context dependent, including costimulation, growth arrest or apoptosis (Jin, Carrio et al., 2004) as well as promoting plasma cell differentiation and supporting antibody class switching (Ozaki et al., 2004, Pene, Gauchat et al., 2004). While IL-21 is known to have a key role in maintaining GC (Linterman, Beaton et al., 2010, Zotos, Coquet et al., 2010), whether any of its multiple

activities contribute to naïve B cell activation and recruitment into the TD B cell response *in vivo* is unresolved. This prompted us to investigate the role of IL-21 during TD B cell response initiation.

Results:

To study the involvement of IL-21 in initiating TD B cell responses, we developed an adoptive transfer and immunization system with defined, identifiable cognate T and B cell partners. WT or *Il21r*$^{-/-}$ mice were crossed with mice that carried a knock-in rearranged BCR specific for hen egg lysozyme (BCR-HEL), known as SW_{HEL} mice (Brink, Paus et al., 2015, Phan, Amesbury et al., 2003). Additionally, these mice were crossed with *eGFP* transgenic mice and onto a *rag1* deficient background to prevent endogenous BCR rearrangement during development and thus unintended B cell activation. In the resultant B cell donor mice, essentially all B cells were specific for HEL (Fig. S1A) and expressed *eGFP* (Fig. S1B). Donor CD4 T cells were derived from mice transgenic for the alpha and beta chains of a CD4 restricted T-cell receptor (TCR) specific for ovalbumin, known as OTII (Barnden, Allison et al., 1998), and carried a *GFP* knock-in at the *Il21* locus, allowing for analysis of *Il21* transcription via GFP fluorescence (Luthje et al., 2012). As an antigen, we generated a recombinant protein of HEL fused with the I-A^{b}-restricted 12-mer peptide recognized by OTII T cells (Robertson, Jensen et al., 2000), referred to as $HEL^{0X}OVA_{pep}$. To study the role of affinity, we introduced 2 or 3 mutations in the sequence encoding HEL, referred to as $HEL^{2X}OVA_{pep}$ and $HEL^{3X}OVA_{pep}$, resulting in a SW_{HEL} BCR affinity series of 2 x 10^{10} M^{-1} (HEL^{0X}), 8 x 10^{7} M^{-1} (HEL^{2x}), and 1.5 x 10^{6} M^{-1} (HEL^{3X}) (Paus, Phan et al., 2006) (Fig. S1C).

IL-21 promotes B cell expansion from the outset of a TD immune response by increasing cell cycle speed and rate of entry.

Having established an experimental system, we first investigated the role of IL-21 in the response to a moderate affinity antigen, $HEL^{2X}OVA_{pep}$. CD45.2 WT and *Il21r*$^{-/-}$, cell-trace violet (CTV) labelled SW_{HEL} B cells (5 x 10^{4} of each) were co-transferred with 5 x 10^{4} *Il21*$^{GFP/+}$ OTII T cells into CD45.1 congenic recipients and immunized *ip* with alum-adsorbed $HEL^{2X}OVA_{pep}$ (Fig. 1A). This setup allowed identification and analysis of WT and *Il21r*$^{-/-}$ SW_{HEL} B cells within the same recipient mouse (Fig. S1D). All SW_{HEL} B cells had started to proliferate at day 3.5 post immunization, but by day 4.5 the expansion of *Il21r*$^{-/-}$ B

cells was reduced significantly compared to their WT counterparts in the same mouse (Fig. 1B). Cell division analysis by CTV dye dilution revealed that over time, *Il21r*$^{-/-}$ B cells were progressively and increasingly disadvantaged, being less likely to enter into subsequent divisions as indicated by an increasing proportion of *Il21r*$^{-/-}$ cells not further diluting CTV (Fig. 1C, D). IL-21 has been implicated in regulating B cell homeostasis by increasing apoptosis in the absence of CD40 signaling in *in vitro* experiments (Mehta, Wurster et al., 2003). To investigate if IL-21 regulated apoptosis during early B cell expansion *in vivo*, we analyzed each CTV peak of WT and *Il21r*$^{-/-}$ SW_{HEL} B cells on day 3.5 post $HEL^{2x}OVA_{pep}$ immunization for the presence of active caspase 3, indicative of the onset of apoptosis. Active caspase 3 positive cells, although rare, were at a similar frequency within each division peak of WT and *Il21r*$^{-/-}$ SW_{HEL} B cells (Fig. 1E), in line with previous reports (Gonzalez et al., 2018).

With cell death an unlikely cause for the reduced representation of *Il21r*$^{-/-}$ SW_{HEL} B cells, we investigated whether IL-21 influenced cell cycle progression. To assess this, S phase cells were time-stamped by incorporation of the DNA nucleoside analogue 5-bromo-2'-deoxyuridine (BrdU), which has a short bioavailability with most labelling occurring within 30 min to 1 hr of injection (Matiasova, Sevc et al., 2014). To track the subsequent progression through the cell cycle, we analyzed the cells' DNA content at various time points thereafter, an approach that has been used to dissect cell cycle progression of T cells (Kretschmer, Flossdorf et al., 2020). Accordingly, cells in active DNA synthesis on day 3.5 post $HEL^{2x}OVA_{pep}$ immunization were labeled with BrdU (Fig. 2A) and analyzed 4, 10 and 12h thereafter. In most instances, a higher proportion of WT SW_{HEL} B cells incorporated BrdU compared to *Il21r*$^{-/-}$ SW_{HEL} B cells in the same animal, confirming that IL-21 increased cell cycle activity (Fig. 2B). To determine if IL-21 enhanced the rate of cell cycle entry, the speed of cell cycle transition or a combination of both, DNA content of $BrdU^{+}$ cells 4, 10 and 12h post BrdU injection was measured by co-staining *ex vivo* with 7-Aminoactinomycin D (7-AAD). Rapidly proliferating B cells have been measured to complete a cell cycle within 8-12h of initiation (Dowling, Kan et al., 2014) with S phase comprising 5-6h (Gitlin et al., 2015), correlating closely with total cell cycle time (Dowling et al., 2014). Therefore, assessing the proportion of $BrdU^{+}$ cells that had completed cell division (that is had 2N DNA content) 4h after BrdU injection allowed us to determine the relative speed of S phase completion and to do so independently of the rate of cell cycle re-entry, as only cells that had completed one S phase were analyzed (Fig. 2C, left). This revealed that the proportion of

$BrdU^+$ cells with 2N DNA content, indicative of the cells having progressed from S to G1 within 4 hours, was significantly higher in WT than *Il21r*$^{-/-}$ SW_{HEL} B cells, indicating more rapid cell cycle progression (Fig. 2D). Ten hours post BrdU injection, twice the time required to complete S phase, a 2N DNA content in $BrdU^+$ cells identified cells that had divided once but not re-entered S phase in a subsequent cell cycle (Fig. 2C, right). The reduced proportion of $BrdU^+$ cells with a 2N DNA content for WT SW_{HEL} B cells compared to *Il21r*$^{-/-}$ B cells indicated a greater fraction of WT SW_{HEL} B cells had re-entered division after 10h, resulting in more cells in S/G2 (Fig. 2D). After 12h, enough time for some cells to have completed 2 rounds of division, 2N DNA content of $BrdU^+$ cells in both genotypes was proportionately similar (Fig. 2D).

The reduced re-entry of cycling *Il21r*$^{-/-}$ SW_{HEL} B cells seen 10 h after the BrdU pulse could be due to increased S phase duration and concomitantly increased cell cycle duration, giving the cells less time from completion to re-entry (Dowling et al., 2014). Equally or additionally, the rate of cell cycle re-entry could be reduced, with the time spent in G1 prolonged, in the absence of IL-21. To investigate if IL-21 influenced the rate of cell cycle initiation, we developed an experimental system in which endogenous IL-21 production and signaling were abrogated (*Il21* and *Il21r* double deficient recipient mice and *Il21*$^{-/-}$ OTII T cells) allowing IL-21 to be provided as a pulse that acted only on the transferred B cells (Fig. 3A). On day 3.5 post cell transfer and immunization, 2 µg of recombinant IL-21 or saline was injected *iv*. Following this, BrdU was injected one hour thereafter to label and exclude cells that had already initiated a cell cycle at the time of IL-21 injection. Consequently, cells that were subsequently $BrdU^-$ were presumed to be in G1 at the time of IL-21 injection. Ten hours after IL-21 injection, the DNA content of $BrdU^-$ cells was analyzed, with cells having >2N DNA content being those that had entered S phase approximately 2-5 hours following IL-21 or saline injection (Fig. 3B). This time point was chosen to allow time for B cells to respond to IL-21 stimulation, complete G1 and enter S phase. To determine the rate of cell cycle entry independent of the extent of cell proliferation by WT and *Il21r*$^{-/-}$ SW_{HEL} B cells over time, the proportion of $BrdU^-$ cells that had entered S phase (DNA content by 7-AAD >2N) was determined for both genotypes (Fig. S1E) and the ratio within each mouse calculated. In the absence of IL-21 injection, the ratio of WT to *Il21r*$^{-/-}$ SW_{HEL} B cells that had entered cell division was randomly distributed. In contrast, following IL-21 administration $BrdU^-$ cells with >2N DNA content, and thus in S/G2, were more frequent among WT cells in all but one

mouse (Fig. 3C). This suggested that promotion of cell cycle entry, in addition to increased S phase speed, was a direct consequence of IL-21 signaling in B cells.

IL-21 synergizes with BCR and CD40 to promote AKT and S6 phosphorylation.

B cell proliferation occurs in the absence of IL-21, indicating that IL-21 amplifies rather than initiates mitogenic signals such as those downstream of either or both BCR and CD40 stimulation. Phosphorylation and activation of AKT, a key event downstream of both BCR and CD40 ligation, can lead to the phosphorylation of mammalian target of rapamycin complex 1 (mTORC1) with the subsequent activation of S6-kinase (S6K) (Luo, Weisel et al., 2018), which in turn regulates key mediators of cell proliferation including phosphorylation of S6 (p-S6). Importantly, IL-21R signaling has been shown to result in AKT phosphorylation (p-AKT) at serine 473 (S473) in cell lines and CD8 T cells (Zeng, Spolski et al., 2007). To explore the possibility that IL-21 promoted the cell cycle via enhancing AKT and S6-phosphoryation, we incubated splenocytes *ex vivo* with or without 20 ng IL-21 for 3 h in the presence of agonistic anti-CD40, also for 3h, or BCR stimulation using biotinylated anti-Igλ/κ followed by streptavidin-mediated cross-linking for the last minute of incubation. Phosphoflow analysis of naïve B cells (Fig. S2A) showed incubation with IL-21 increased AKT phosphorylation at S473, which was further increased by co-stimulation through BCR or CD40 (Fig. 4A, B). IL-21R dependency was confirmed with B cells from *Il21r*$^{-/-}$ mice, which retained AKT phosphorylation in response to BCR or CD40 stimulation but were unaffected by exposure to IL-21 (Fig. 4A, B). Phosphorylation of S6 was minimally induced following BCR ligation and more so following CD40 stimulation but potently increased by the presence of IL-21 (Fig. 4C). p-S6 amounts were distributed bimodally with the frequency of p-S6 positive cells increased by exposure to IL-21, and further again by addition of BCR or CD40 signals (Fig. 4D), effects that also required IL-21R expression (Fig. 4C, D). In addition to increasing the proportion of p-S6 positive cells, IL-21 increased the median amount of p-S6 among p-S6 positive cells (Fig. 4E).

T cell help via CD40 ligation is essential for T-dependent immune responses *in vivo(Kawabe, Naka et al., 1994)* and the observed additive signaling suggested that IL-21 may change the minimal CD40 signaling threshold and/or amplify the response to CD40 ligation. To test this, we cultured CTV labeled naïve SW_{HEL} B cells with or without 10, 1, 0.1 µg anti-CD40 and in the presence or absence of IL-21 (20 ng/ml) and analyzed CTV dilution three days thereafter. As expected, the initiation of proliferation was dependent on CD40 signaling in a dose-

dependent manner (Fig. 4F). The presence of IL-21 increased the extent of CTV dilution and, at the lowest concentration of anti-CD40, CTV dilution was dependent on IL-21 (Fig. 4F). Collectively, these results indicated that IL-21 amplified BCR and CD40 signaling and lowered the minimal T cell help requirement for cell cycle initiation.

IL-21 modulates the BCR affinity threshold for response recruitment.

The increased initiation and expedited progression through division in response to IL-21 and the amplification of p-S6 signaling suggested a role for IL-21 in the recruitment of B cells into accruing GC responses. Moreover, with T cell help to B cells being determined by the efficiency of antigen capture and presentation in the context of MHC-II (Schwickert et al., 2011, Woodruff, Kim et al., 2018), the reduced anti-CD40 requirement for cell cycle initiation in the presence of IL-21 *in vitro* suggested that IL-21 may influence the BCR affinity threshold for response participation *in vivo*. To investigate the contribution of IL-21 and BCR affinity *in vivo*, we immunized mice with HEL^{0X}-, HEL^{2X}- or HEL^{3X}-OVA_{pep} adsorbed on 45 µg alum adjuvant and analyzed the SW_{HEL} B and OTII T cell response 4.5 days post immunization (Fig 5A). For the lowest affinity antigen (HEL^{3x}-OVA_{pep}) we also included a group receiving 90 µg of alum. The number of $Il21^{GFP/+}$ OTII cells that differentiated into $CXCR5^{+}$ $PD\text{-}1^{high}$ Tfh cells (Fig. S2B), was independent of the HEL-OVA_{pep} variant used with a statistically non-significant tendency towards higher cell numbers if 90 µg adjuvant was used (Fig. 5B). Similarly, the proportion of $Il21^{GFP/+}$ OTII Tfh expressing GFP and thus transcribing the *Il21* locus, was comparable (Fig. 5C). Thus, early Tfh differentiation and IL-21 production were largely independent of the HEL-OVA_{pep} antigen variant used, effectively creating an experimental system in which the presence or absence of IL-21 signaling to B cells, BCR affinity and adjuvant dose were the only variables. Cell division was monitored by CTV dye dilution of SW_{HEL} B cells, done using spectral cytometry that provided an increased resolution of 9 divisions (peak 0 to 9+, Fig. S2C and 5D). SW_{HEL} B cells showed reduced proliferation in the absence of IL-21R signaling at each BCR affinity and adjuvant dose (Fig. 5D). The extent of the deficiency increased with reduced affinity - HEL^{3X}-OVA immunized mice showing almost no participation of $Il21r^{-/-}$ SW_{HEL} B cells (Fig. 5D). To compare distributions of undivided, minimally proliferative, moderately proliferative and highly proliferative cells, we classified cells into CTV peaks 0, 1-4, 4-8 and 9+, respectively. Across all immunizations, a significantly higher proportion of WT SW_{HEL} B cells were present within peak 9+, indicating

more extensive proliferation. In contrast, $HEL^{3x}OVA_{pep}$ immunizations resulted in the majority of *Il21r* $^{-/-}$ B cells remaining undivided and thus in CTV peak 0 (Fig. 5E). The ratio (Fig. 5F) and cell count (Fig. 5G) of pooled WT and *Il21r* $^{-/-}$ B cells within each CTV peak further highlighted the BCR-affinity dependence of the IL-21 mediated response amplification, and indicated that the magnitude of the deficiency in proliferation conferred by IL-21R deficiency was exaggerated as cells divided more. Indeed, while the overall trends were maintained across all experimental groups, and affirming the proportionality data, analysis of pooled CTV peak cell counts showed that $HEL^{3x}OVA_{pep}$ immunization resulted in significantly more *Il21r* $^{-/-}$ B cells in CTV peak 0 independent of adjuvant dose, indicating reduced recruitment into the response (Fig. 5H). In contrast, CTV peaks 5-8 and 9+ were dominated by WT cells (Fig. 5H). Thus, IL-21 promoted early B cell expansion, particularly of B cells with low affinity for antigen, and did so from the very onset of the response by increasing participation and sustaining continued proliferation.

Discussion:

The results reported here show IL-21R signaling to be a crucial component of early B cell activation during TD B cell responses, promoting B cell expansion by increasing the speed of cell cycle transition and the rate of entry and re-entry into the cell cycle. These effects are most prominent for B cells with low affinity for antigen and are mediated, at least in part, by IL-21 and T cell help additively promoting two key events in triggering cell division, phosphorylation of AKT and S6. Signaling via JAK-STAT, in particular STAT3, is activated downstream of the IL21-R and its absence results in reduced proliferation and increased apoptosis in the presence of CD40 ligation of human B cells (Avery, Deenick et al., 2010). Furthermore, IL-21R signaling results in PI3K and MAPK activation and promotes cell division by inducing S6 phosphorylation (reviewed (Leonard & Wan, 2016)) and IL21 was recently reported to promote GC B cell proliferation by sustaining the c-MYC target AP4 (Chou, Verbaro et al., 2016). BCR and CD40 employ PI3K and NF-kB pathways to transduce activating signals in B cells that, depending on signal duration and magnitude, can also result in the phosphorylation of S6 (Luo et al., 2018). The convergence of proliferation-inducing pathways on p-S6 allows IL-21 to promote B cell proliferation either by increasing the basal p-S6 amount or by increasing activation in conjunction with BCR or CD40 signaling. BCR signaling in naïve B cells was shown to be increased compared to GC B cells (Khalil, Cambier et al., 2012), particularly NF-kB signaling (Luo et al., 2018, Nowosad,

Spillane et al., 2016). As a result, the strength of BCR signaling, determined by the affinity for antigen (Liu et al., 2010), strongly influences their activation. The initiation of the cell cycle in naïve B cells is a multi-step process in which BCR signaling changes the metabolic state of the cell but is, by itself, insufficient to initiate the cell cycle (Akkaya, Traba et al., 2018). Subsequent, timely receipt of T cell help then induces the commencement of proliferation (Akkaya et al., 2018). Antigen affinity therefore regulates B cell response initiation via BCR signaling and by determining the efficiency of antigen uptake und thus the receptiveness to T cell help (Schwickert et al., 2011). However, the magnitude and breadth of a B cell response is also related to the inflammatory stimuli delivered by vaccination or infection. The production of cytokines by CD4 T cells is one way by which information about the nature of an infection is conveyed to B cells, resulting for example in differential antibody isotype class-switch recombination (McIntyre, Klinman et al., 1993, Reinhardt, Liang et al., 2009, Snapper et al., 1988). The results presented here reveal an additional way by which T cells regulate B cell responses, this being IL-21 mediated modulation of naïve B cell recruitment and their subsequent proliferation, but importantly influenced by BCR affinity and likely associated with differential acquisition of T cell help. IL-21 production by CD4 T cells is induced by IL-6 (Dienz, Eaton et al., 2009, Suto, Kashiwakuma et al., 2008) and calcium signaling via NFAT (Kim, Korn et al., 2005, Mehta, Wurster et al., 2005) and thus in response to inflammatory signaling with a STAT3-dependent autocrine loop stabilizing its production (Caprioli, Sarra et al., 2008). This enables IL-21 to fine-tune B cell responses in relation to immunological parameters of the immunogen. Conversely, excessive IL-21 production could result in the potentially detrimental lowering of BCR signaling thresholds and thus predispose to autoimmunity. This could provide a mechanistic explanation for the association of polymorphisms in *Il21* and *Il21r* (Sawalha, Kaufman et al., 2008, Webb, Merrill et al., 2009) and increased IL-21 production (Dolff, Abdulahad et al., 2011) with systemic lupus erythematosus (SLE).

In summary, by lowering the BCR affinity threshold for naïve B cell recruitment into T-dependent B cell responses and increasing both cell cycle initiation and speed, IL-21 modulates the breath and magnitude of GC initiation. These results provide a novel mechanism by which IL-21 influences responses to vaccination and infection and reveal new insights into its potential involvement in autoimmunity.

Materials and methods:

Mice, cell transfer and immunization.

SW_{HEL} mice (V_H10_{tar}IgH, Vκ10-κ Tg) (Phan et al., 2003) were crossed with *Rag*$1^{-/-}$ (L. Corcoran, WEHI, Australia) and *Il21r*$^{-/-}$ mice (W. Leonard, NIH, USA). OTII mice (Barnden et al., 1998) (W. Heath, University of Melbourne, Australia) were crossed with *Il21 GFP* knock-in mice (Luthje et al., 2012) to obtain IL-21-GFP reporter mice (*Il21*$^{GFP/+}$) or IL-21 deficient mice (*Il21*$^{GFP/GFP}$, referred to as *Il21*$^{-/-}$). All mice were bred under specific pathogen free conditions within the Monash Animal Research Platform and the ARA Animal Ethics Committee (Application E/1787/2018/M) approved all animal studies.

For adoptive cell transfer, spleens of OTII and SW_{HEL} mice were passed through a 70 µM mesh, red blood cells lysed, and the frequency of T and B cells determined by flow cytometry. Additionally, B cells were depleted from OTII splenocytes by magnetic sorting using CD45R (B220) MicroBeads according manufacturer's instructions (Miltenyi Biotec cat. 130-049-501). For experiments involving cell division analysis, SW_{HEL} B cells were labelled with CTV (Thermo Fisher cat. C34557) according to the manufacturer's instructions. Per recipient mouse, a mix of 1 x 10^5 SW_{HEL} (50 % WT, 50 % *Il21r*$^{-/-}$) and 5 x 10^4 OTII T cells was then transferred *iv* and mice were immunized *ip* with 50 µg $HEL^{0X}OVA_{pep}$, $HEL^{2X}OVA_{pep}$ or $HEL^{3X}OVA_{pep}$ adsorbed on 45 or 90 µg alum adjuvant (Alhydrogel, InvivoGen cat. 21645-51-2).

HEL-OVA$_{pep}$ protein production.

The nucleic acid sequence of HEL, HEL^{2X} (HEL with D101R and R73E mutations (Brink, Phan et al., 2008)) or HEL^{3X} (HEL with D101R, R73E and R21Q mutations (Brink et al., 2008)) fused to $OVA_{217-345}$ and a deka-HIS tag was cloned into the pcDNA3.1 plasmid. Expi293 or HEK293E cells were transfected using polyethyleneimine (PEI) following culture for 5 days. TALON Superflow Metal Affinity Resin (Takarabio cat. 635506) was used to purify the recombinant HEL-OVA_{pep} protein. After dialysis against PBS, and concentration to 0.8-1.2 mg/mL (Amicon Ultra-15 Centrifugal Filter Units, Merck cat. UFC901024), the final protein was analyzed by polyacrylamide gel electrophoresis and Coomassie blue staining, aliquoted and frozen at -80°C.

Flow cytometry.

Spleens were isolated and passed through a 70µM mesh to generate a single cell suspension. Following red-blood cell lysis, up to 5 x 10^7 cells were stained with monoclonal antibodies (Table 1) to cell surface proteins and biotinylated HEL-OVA diluted in PBS containing 1 % BSA (Bovogen) and 0.1 % NaN_3 (Sigma) and in the presence of FcγR blocking antibody (clone 2.4G2, WEHI Antibody Facility) and 1 % rat serum on ice for 30 minutes. Dead cells were excluded using Fixable Viability Dye eFluor™ 780 (eBioscience, cat. 65-0865-14) or FluoroGold (Santa Cruz Biotechnology, CAS 223769-64-0). Cells were analyzed using BD LSR Fortessa X-20, BD LSR-II or Cytek Aurora flow cytometers. The data were analyzed with FlowJo (BD) and SpectroFlo (Cytek) software and statistical analysis was performed using Prism 8 (GraphPad).

Table 1: Monoclonal antibodies, lectins and streptavidins used for flow cytometry.

Antibody or lectin	**Source**	**Identifier**
Active Caspase 3-BV650 (clone C92-605)	BD Biosciences	564096
B220-BV421 (clone RA3-B62)	BD Biosciences	562922
B220-PerCP-Cy5.5 (clone RA3-B62)	BD Biosciences	551960
BrdU-AF647 (clone 3D4)	BD Biosciences	560209
CD16/32 (clone 2.4G2)	WEHI Antibody Facility	N/A
CD4-A680 (clone GK1.5)	WEHI Antibody Facility	N/A
CD4-PerCP-Cy5.5 (clone RM4-5)	BD Biosciences	550954
CD19-BUV737 (clone 1D3)	BD Biosciences	612781
CD45.1-APC-eFluor780 (clone A20)	Invitrogen	47053-82
CD45.1- PerCP-Cy5.5 (clone A20)	eBioscience	45-0453-80
CD45.2-BV786 (clone 104)	BD Biosciences	563686
CXCR5-Biotin (clone 2G8)	BD Biosciences	551960
FAS-BUV395 (clone Jo2)	BD Biosciences	740254
IgD-BV711 (clone 11-26c.2a)	BD Biosciences	564275
p-AKT (S473)-PE (clone M89-61)	BD Biosciences	561671
PD-1-PE (clone J43)	BD Biosciences	551892
PNA-FITC	Vector Laboratories	FL-1071

p-S6 (Ser235/236)-PE-Cy7 (clone D57.2.2E)	Cell Signaling	34411S
Streptavidin-PE-Cy7	eBioscience	25-4317-82
Streptavidin-BV650	BD Biosciences	563855
Streptavidin-BV786	BD Biosciences	563858
TCR-Vα2-APC (clone B20.1)	WEHI Antibody Facility	N/A
TCR-Vβ5.1, 5.2-PE-Cy7 (clone MR9-4)	BioLegend	139508

BrdU incorporation and 7AAD staining.

For *in vivo* BrdU incorporation, mice were injected *ip* with 200 µL of 10 mg/mL 5-bromo-2'-deoxyuridine (BrdU, BD cat. 559619). Mice were culled by cervical dislocation at the time point indicated in the individual experimental setup, spleens were harvested, and 6 x 10^7 cells stained with monoclonal antibodies against cell-surface molecules as described above. After washing with FACS buffer, cells were suspended in 200 µL BD Cytofix/Cytoperm (BD cat. 554722) and incubated for 15 min on ice followed by washing with 2 mL BD Perm/Wash. If staining for active caspase-3, the cells were then incubated for 30 min with anti-active caspase 3 in BD Perm/Wash (BD cat. 554723). Next, cells were suspended in 150 µL BD Permeabilization Buffer Plus (BD cat. 561651) on ice for 10 min followed by washing with 2 mL BD Perm/Wash. Cells were fixed again with 150 µL BD Cytofix/Cytoperm on ice for 5 min followed by washing with 2 mL BD Perm/Wash. To increase BrdU accessibility for monoclonal antibodies, DNAse digest was performed. Per sample a mix of 60 µL DNAse1 stock (1 mg/mL in ddH_2O, Sigma, Cat. D4513) and 140 µL PBS was freshly prepared and cells were incubated at 37°C for 1 h. After washing with 1 mL BD Perm/Wash, cells were incubated at room temperature with fluorochrome labelled anti-BrdU diluted in BD Perm/Wash. After a final wash with 2 mL BD Perm/Wash, cells were either resuspended in 1 mL FACS buffer or incubated with 20 µL 7-AAD for 5 minutes followed by the addition of 1 mL FACS buffer and acquired as described above.

In vitro cell culture, stimulation and phosphoflow staining.

For phosphoflow analysis, splenocytes were isolated from C57Bl/6 and *Il21r*$^{-/-}$ mice and 3 x 10^6 cells used per stimulation condition. Cells were incubated for 3 hours at 37°C in RPMI media supplemented with or without recombinant mouse IL-21 (20 ng/mL, Peprotech cat. 210-21-100). Cells were stimulated with either anti-Igκ and anti-Igλ or anti-CD40. For anti-

Igκ and anti-Igλ stimulation, biotinylated rat anti-Igκ (100 ng/mL; clone 187.1, WEHI Antibody Facility) and anti-Igλ (100 ng/mL; clone JC5, WEHI Antibody Facility) were added during the final 15 min of the 3h incubation, followed by addition of avidin (10 µg/mL) for 1 min. For anti-CD40 stimulation, cells were incubated with anti-CD40 (20 ng/mL; clone 1C10, WEHI Antibody Facility) throughout the 3h culture period. Stimulation was stopped by fixation and permeabilization with the BD phosphoflow staining reagents (BD cat. 558049 and 558050) as per manufacturer's instructions. Cells were stained for flow cytometry with anti-p-AKT, anti-p-S6, anti-B220, anti-IgD and PNA (see Table 1 for further details). Flow cytometry was performed on a LSRFortessa X20 flow cytometer (BD). Flow cytometry data were analyzed with FlowJo 10 software (BD). For *in vitro* cell culture of SW_{HEL} B cells, 1 x 10^6 splenocytes from a $RAG^{-/-}$ SW_{HEL} mouse were incubated per well of a 96-well U-bottom plate in RPMI media supplemented with 5 % fetal calf serum, 1 µg/ml HEL-OVA, IL-4 (10 ng/ml) and additional stimuli as indicated.

Statistical analysis.

All statistical analysis was performed using Prism 8 (GraphPad). Mice failing to respond to immunization, as evidenced by failure to expand adoptively transferred B cells, were excluded from analysis. In experiments where the expansion of WT and *Il21r*$^{-/-}$ B cells was studied within the same animal, cell counts were corrected for any deviation of a 1:1 ratio at the time of transfer.

Author contributions:

Conceptualization: DMT, IQ; Methodology: ARD, CIM, RB, DZ, IQ; Investigation: ARD, CIM, MJR, ZD, CP, KOD, IQ; Writing- Original Draft: IQ; Writing- Review and Editing: ARD, CIM, MJR, ZD, DZ, RB, DMT, IQ.

Acknowledgements:

We thank Lynn M. Corcoran, William R. Heath, Warren J. Leonard and Stephen L. Nutt for providing mouse strains. We thank the Alfred Alliance Monash Intensive Care Unit, and Monash Animal Research Platform for animal husbandry and Stephanie Jansen for assistance with intravenous injections. The authors acknowledge the contributions of AMREPflow,

Noelene Quinsey from the Monash Protein Production Unit; Tim Adams, Tam Pham, Tram Phan and George Lovercz from the Commonwealth Scientific and Industrial Research Organisation (CSIRO). A.R.D was supported by a Monash University Research Training Program (RTP) Stipend and Z.D. by a Swedish International Postdoctoral Fellowship (2016-06659). D.M.T. was funded by National Health and Medical Research Council (NHMRC) Australia Investigator Award (APP1175411), I.Q. by an Early Postdoc Mobility fellowship (P2ZHP3_164964) and an Advanced Postdoc Mobility fellowship (P300PA_177893) provided by the Swiss National Science Foundation and a Peter Doherty Early Career fellowship (APP1145136) provided by NHMRC Australia. This work was supported by NHMRC Project Grant APP1146617 awarded to D.M.T, D.Z and I.Q, Monash Platform Access grants PAG17-0207 awarded to D.Z, I.Q and D.M.T and PAG18-0409 awarded to I.Q. and D.Z, NHMRC Ideas Grants APP1185294 awarded to M.J.R and I.Q. and APP2002393 awarded to I.Q.

References:

Akkaya M, Traba J, Roesler AS, Miozzo P, Akkaya B, Theall BP, Sohn H, Pena M, Smelkinson M, Kabat J, Dahlstrom E, Dorward DW, Skinner J, Sack MN, Pierce SK (2018) Second signals rescue B cells from activation-induced mitochondrial dysfunction and death. *Nat Immunol*

Allen CD, Okada T, Tang HL, Cyster JG (2007) Imaging of germinal center selection events during affinity maturation. *Science* 315: 528-31

Avery DT, Deenick EK, Ma CS, Suryani S, Simpson N, Chew GY, Chan TD, Palendira U, Bustamante J, Boisson-Dupuis S, Choo S, Bleasel KE, Peake J, King C, French MA, Engelhard D, Al-Hajjar S, Al-Muhsen S, Magdorf K, Roesler J et al. (2010) B cell-intrinsic signaling through IL-21 receptor and STAT3 is required for establishing long-lived antibody responses in humans. *J Exp Med* 207: 155-71

Barnden MJ, Allison J, Heath WR, Carbone FR (1998) Defective TCR expression in transgenic mice constructed using cDNA-based alpha- and beta-chain genes under the control of heterologous regulatory elements. *Immunol Cell Biol* 76: 34-40

Brink R, Paus D, Bourne K, Hermes JR, Gardam S, Phan TG, Chan TD (2015) The SW(HEL) system for high-resolution analysis of in vivo antigen-specific T-dependent B cell responses. *Methods Mol Biol* 1291: 103-23

Brink R, Phan TG, Paus D, Chan TD (2008) Visualizing the effects of antigen affinity on T-dependent B-cell differentiation. *Immunol Cell Biol* 86: 31-39

Caprioli F, Sarra M, Caruso R, Stolfi C, Fina D, Sica G, MacDonald TT, Pallone F, Monteleone G (2008) Autocrine regulation of IL-21 production in human T lymphocytes. *J Immunol* 180: 1800-7

Chou C, Verbaro DJ, Tonc E, Holmgren M, Cella M, Colonna M, Bhattacharya D, Egawa T (2016) The Transcription Factor AP4 Mediates Resolution of Chronic Viral Infection through Amplification of Germinal Center B Cell Responses. *Immunity* 45: 570-582

Chtanova T, Tangye SG, Newton R, Frank N, Hodge MR, Rolph MS, Mackay CR (2004) T follicular helper cells express a distinctive transcriptional profile, reflecting their role as non-Th1/Th2 effector cells that provide help for B cells. *J Immunol* 173: 68-78

Dienz O, Eaton SM, Bond JP, Neveu W, Moquin D, Noubade R, Briso EM, Charland C, Leonard WJ, Ciliberto G, Teuscher C, Haynes L, Rincon M (2009) The induction of antibody production by IL-6 is indirectly mediated by IL-21 produced by CD4+ T cells. *J Exp Med* 206: 69-78

Dolff S, Abdulahad WH, Westra J, Doornbos-van der Meer B, Limburg PC, Kallenberg CG, Bijl M (2011) Increase in IL-21 producing T-cells in patients with systemic lupus erythematosus. *Arthritis Res Ther* 13: R157

Dowling MR, Kan A, Heinzel S, Zhou JH, Marchingo JM, Wellard CJ, Markham JF, Hodgkin PD (2014) Stretched cell cycle model for proliferating lymphocytes. *Proc Natl Acad Sci U S A* 111: 6377-82

Ford D, Sheehan C, Girasole C, Priester R, Kouttab N, Tigges J, King TC, Luciani A, Morgan JW, Maizel AL (1999) The human B cell response to IL-13 is dependent on cellular phenotype as well as mode of activation. *J Immunol* 163: 3185-93

Gitlin AD, Mayer CT, Oliveira TY, Shulman Z, Jones MJ, Koren A, Nussenzweig MC (2015) HUMORAL IMMUNITY. T cell help controls the speed of the cell cycle in germinal center B cells. *Science* 349: 643-6

Gonzalez DG, Cote CM, Patel JR, Smith CB, Zhang Y, Nickerson KM, Zhang T, Kerfoot SM, Haberman AM (2018) Nonredundant Roles of IL-21 and IL-4 in the Phased Initiation of Germinal Center B Cells and Subsequent Self-Renewal Transitions. *J Immunol* 201: 3569-3579

Good KL, Bryant VL, Tangye SG (2006) Kinetics of human B cell behavior and amplification of proliferative responses following stimulation with IL-21. *J Immunol* 177: 5236-47

Jin H, Carrio R, Yu A, Malek TR (2004) Distinct activation signals determine whether IL-21 induces B cell costimulation, growth arrest, or Bim-dependent apoptosis. *J Immunol* 173: 657-65

Kato Y, Abbott RK, Freeman BL, Haupt S, Groschel B, Silva M, Menis S, Irvine DJ, Schief WR, Crotty S (2020) Multifaceted Effects of Antigen Valency on B Cell Response Composition and Differentiation In Vivo. *Immunity*

Kawabe T, Naka T, Yoshida K, Tanaka T, Fujiwara H, Suematsu S, Yoshida N, Kishimoto T, Kikutani H (1994) The immune responses in CD40-deficient mice: impaired immunoglobulin class switching and germinal center formation. *Immunity* 1: 167-78

Khalil AM, Cambier JC, Shlomchik MJ (2012) B cell receptor signal transduction in the GC is short-circuited by high phosphatase activity. *Science* 336: 1178-81

Kim HP, Korn LL, Gamero AM, Leonard WJ (2005) Calcium-dependent activation of interleukin-21 gene expression in T cells. *J Biol Chem* 280: 25291-7

Kim YM, Pan JY, Korbel GA, Peperzak V, Boes M, Ploegh HL (2006) Monovalent ligation of the B cell receptor induces receptor activation but fails to promote antigen presentation. *Proc Natl Acad Sci U S A* 103: 3327-32

Kretschmer L, Flossdorf M, Mir J, Cho YL, Plambeck M, Treise I, Toska A, Heinzel S, Schiemann M, Busch DH, Buchholz VR (2020) Differential expansion of T central memory precursor and effector subsets is regulated by division speed. *Nat Commun* 11: 113

Leonard WJ, Wan CK (2016) IL-21 Signaling in Immunity. *F1000Res* 5

Linterman MA, Beaton L, Yu D, Ramiscal RR, Srivastava M, Hogan JJ, Verma NK, Smyth MJ, Rigby RJ, Vinuesa CG (2010) IL-21 acts directly on B cells to regulate Bcl-6 expression and germinal center responses. *J Exp Med* 207: 353-63

Liu W, Meckel T, Tolar P, Sohn HW, Pierce SK (2010) Antigen affinity discrimination is an intrinsic function of the B cell receptor. *J Exp Med* 207: 1095-111
Luo W, Weisel F, Shlomchik MJ (2018) B Cell Receptor and CD40 Signaling Are Rewired for Synergistic Induction of the c-Myc Transcription Factor in Germinal Center B Cells. *Immunity* 48: 313-326 e5
Luthje K, Kallies A, Shimohakamada Y, Belz GT, Light A, Tarlinton DM, Nutt SL (2012) The development and fate of follicular helper T cells defined by an IL-21 reporter mouse. *Nat Immunol* 13: 491-8
Matiasova A, Sevc J, Mikes J, Jendzelovsky R, Daxnerova Z, Fedorocko P (2014) Flow cytometric determination of 5-bromo-2'-deoxyuridine pharmacokinetics in blood serum after intraperitoneal administration to rats and mice. *Histochem Cell Biol* 142: 703-12
McIntyre TM, Klinman DR, Rothman P, Lugo M, Dasch JR, Mond JJ, Snapper CM (1993) Transforming growth factor beta 1 selectivity stimulates immunoglobulin G2b secretion by lipopolysaccharide-activated murine B cells. *J Exp Med* 177: 1031-7
Mehta DS, Wurster AL, Weinmann AS, Grusby MJ (2005) NFATc2 and T-bet contribute to T-helper-cell-subset-specific regulation of IL-21 expression. *Proc Natl Acad Sci U S A* 102: 2016-21
Mehta DS, Wurster AL, Whitters MJ, Young DA, Collins M, Grusby MJ (2003) IL-21 induces the apoptosis of resting and activated primary B cells. *J Immunol* 170: 4111-8
Mesin L, Ersching J, Victora GD (2016) Germinal Center B Cell Dynamics. *Immunity* 45: 471-82
Niiro H, Clark EA (2002) Regulation of B-cell fate by antigen-receptor signals. *Nat Rev Immunol* 2: 945-56
Nowosad CR, Spillane KM, Tolar P (2016) Germinal center B cells recognize antigen through a specialized immune synapse architecture. *Nat Immunol* 17: 870-7
Ozaki K, Spolski R, Ettinger R, Kim HP, Wang G, Qi CF, Hwu P, Shaffer DJ, Akilesh S, Roopenian DC, Morse HC, 3rd, Lipsky PE, Leonard WJ (2004) Regulation of B cell differentiation and plasma cell generation by IL-21, a novel inducer of Blimp-1 and Bcl-6. *J Immunol* 173: 5361-71
Paus D, Phan TG, Chan TD, Gardam S, Basten A, Brink R (2006) Antigen recognition strength regulates the choice between extrafollicular plasma cell and germinal center B cell differentiation. *J Exp Med* 203: 1081-91
Pene J, Gauchat JF, Lecart S, Drouet E, Guglielmi P, Boulay V, Delwail A, Foster D, Lecron JC, Yssel H (2004) Cutting edge: IL-21 is a switch factor for the production of IgG1 and IgG3 by human B cells. *J Immunol* 172: 5154-7
Phan TG, Amesbury M, Gardam S, Crosbie J, Hasbold J, Hodgkin PD, Basten A, Brink R (2003) B cell receptor-independent stimuli trigger immunoglobulin (Ig) class switch recombination and production of IgG autoantibodies by anergic self-reactive B cells. *J Exp Med* 197: 845-60
Qi H, Cannons JL, Klauschen F, Schwartzberg PL, Germain RN (2008) SAP-controlled T-B cell interactions underlie germinal centre formation. *Nature* 455: 764-9
Reinhardt RL, Liang HE, Locksley RM (2009) Cytokine-secreting follicular T cells shape the antibody repertoire. *Nat Immunol* 10: 385-93
Robertson JM, Jensen PE, Evavold BD (2000) DO11.10 and OT-II T cells recognize a C-terminal ovalbumin 323-339 epitope. *J Immunol* 164: 4706-12
Robinson MJ, Pitt C, Brodie EJ, Valk AM, O'Donnell K, Nitschke L, Jones S, Tarlinton DM (2019) BAFF, IL-4 and IL-21 separably program germinal center-like phenotype acquisition, BCL6 expression, proliferation and survival of CD40L-activated B cells in vitro. *Immunol Cell Biol* 97: 826-839

Sawalha AH, Kaufman KM, Kelly JA, Adler AJ, Aberle T, Kilpatrick J, Wakeland EK, Li QZ, Wandstrat AE, Karp DR, James JA, Merrill JT, Lipsky P, Harley JB (2008) Genetic association of interleukin-21 polymorphisms with systemic lupus erythematosus. *Ann Rheum Dis* 67: 458-61

Schwickert TA, Victora GD, Fooksman DR, Kamphorst AO, Mugnier MR, Gitlin AD, Dustin ML, Nussenzweig MC (2011) A dynamic T cell-limited checkpoint regulates affinity-dependent B cell entry into the germinal center. *J Exp Med* 208: 1243-52

Shih TA, Meffre E, Roederer M, Nussenzweig MC (2002) Role of BCR affinity in T cell dependent antibody responses in vivo. *Nat Immunol* 3: 570-5

Snapper CM, Finkelman FD, Stefany D, Conrad DH, Paul WE (1988) IL-4 induces co-expression of intrinsic membrane IgG1 and IgE by murine B cells stimulated with lipopolysaccharide. *J Immunol* 141: 489-98

Spillane KM, Tolar P (2017) B cell antigen extraction is regulated by physical properties of antigen-presenting cells. *J Cell Biol* 216: 217-230

Suto A, Kashiwakuma D, Kagami S, Hirose K, Watanabe N, Yokote K, Saito Y, Nakayama T, Grusby MJ, Iwamoto I, Nakajima H (2008) Development and characterization of IL-21-producing CD4+ T cells. *J Exp Med* 205: 1369-79

Tangye SG, Avery DT, Hodgkin PD (2003) A division-linked mechanism for the rapid generation of Ig-secreting cells from human memory B cells. *J Immunol* 170: 261-9

Wagner EF, Hanna N, Fast LD, Kouttab N, Shank PR, Vazquez A, Sharma S (2000) Novel diversity in IL-4-mediated responses in resting human naive B cells versus germinal center/memory B cells. *J Immunol* 165: 5573-9

Webb R, Merrill JT, Kelly JA, Sestak A, Kaufman KM, Langefeld CD, Ziegler J, Kimberly RP, Edberg JC, Ramsey-Goldman R, Petri M, Reveille JD, Alarcon GS, Vila LM, Alarcon-Riquelme ME, James JA, Gilkeson GS, Jacob CO, Moser KL, Gaffney PM et al. (2009) A polymorphism within IL21R confers risk for systemic lupus erythematosus. *Arthritis Rheum* 60: 2402-7

Woodruff MC, Kim EH, Luo W, Pulendran B (2018) B Cell Competition for Restricted T Cell Help Suppresses Rare-Epitope Responses. *Cell Rep* 25: 321-327 e3

Zaretsky I, Atrakchi O, Mazor RD, Stoler-Barak L, Biram A, Feigelson SW, Gitlin AD, Engelhardt B, Shulman Z (2017) ICAMs support B cell interactions with T follicular helper cells and promote clonal selection. *J Exp Med* 214: 3435-3448

Zeng R, Spolski R, Casas E, Zhu W, Levy DE, Leonard WJ (2007) The molecular basis of IL-21-mediated proliferation. *Blood* 109: 4135-42

Zhang Y, Tech L, George LA, Acs A, Durrett RE, Hess H, Walker LSK, Tarlinton DM, Fletcher AL, Hauser AE, Toellner KM (2018) Plasma cell output from germinal centers is regulated by signals from Tfh and stromal cells. *J Exp Med* 215: 1227-1243

Zotos D, Coquet JM, Zhang Y, Light A, D'Costa K, Kallies A, Corcoran LM, Godfrey DI, Toellner KM, Smyth MJ, Nutt SL, Tarlinton DM (2010) IL-21 regulates germinal center B cell differentiation and proliferation through a B cell-intrinsic mechanism. *J Exp Med* 207: 365-78

Zotos D, Tarlinton DM (2012) Determining germinal centre B cell fate. *Trends Immunol* 33: 281-8

Declaration of interests:

The authors declare that they have no conflict of interest.

Figure legends:

Fig. 1: IL-21 promotes B cell expansion.

(A) Experimental setup to study expansion of WT and *Il21r*$^{-/-}$ SW_{HEL} B cells. **(B)** Ratio of WT to *Il21r*$^{-/-}$ splenic SW_{HEL} B cells over time and **(C)** representative data showing cell ratio within CTV division peaks and **(D)** CTV profile on day 3.5 with graphs depicting pooled, concatenated data of 4-5 mice per time point. **(E)** Rate of apoptosis measured by detecting active caspase 3 by flow cytometry. Pooled data from 4 mice, representative for 2 experiments. Statistical analysis by one-way ANOVA with Tukey's post-test.

Fig. 2: IL-21 increases cell cycle speed and rate of re-entry.

(A) Experimental setup of BrdU pulse on day 3.5 post immunization. **(B)** WT to *Il21r*$^{-/-}$ SW_{HEL} B cell ratio of cells that have been in S phase and thus incorporated BrdU (pooled data from 4, 10 and 12h time points). **(C)** Schematic depiction of BrdU and DNA content (7AAD) analysis. At 4h, BrdU positive cells with 2N DNA content mark those that have finished the cell cycle, whereas at 10h 2N DNA content identifies cells that have not yet entered the subsequent cell cycle. **(D)** Ratio of the proportion of BrdU positive WT and *Il21r*$^{-/-}$ SW_{HEL} B cells with 2N DNA content on day 3.5 post immunization and 4, 10 and 12h post BrdU pulse. Statistical analysis by one-sample t test.

Fig. 3: IL-21 directly promotes cell cycle entry.

(A) Experimental setup of *in vivo* IL-21 pulse. **(B)** Schematic depiction of BrdU and 7AAD analysis. Cells that had not already been in or were about to enter S phase at the time of IL-21 treatment were identified as being BrdU negative. > 2N DNA content among BrdU negative cells marked those that have entered the cell cycle following saline or IL-21 treatment. **(C)** Rate of *de novo* cell cycle entry 10h post *in vivo* IL-21 (2 µg) or saline pulse. The ratio of the fraction of WT to *Il21r*$^{-/-}$ cells not in S/G2 at the time of pulse ($BrdU^-$ cells) and containing >2N DNA content 10h after pulse is shown. All data were pooled from two independent experiments unless otherwise specified. Statistical analysis by one-sample t test.

Fig. 4: IL-21 synergizes with BCR and CD40 to promote AKT and S6 phosphorylation.

(A-E) Phosphoflow analysis of naïve WT or *Il21r*$^{-/-}$ B cells following *in vitro* culture for 3h with or without IL-21 (20 ng/ml) and/or in the presence of BCR cross-linking (biotinylated

anti-Igκ + anti-Igλ and avidin-mediated cross-linking) or agonistic anti-CD40. **(A)** Exemplary p-AKT (S473) staining and **(B)** quantification of median fluorescence intensity (MFI). **(C)** Exemplary p-S6 (Ser235/236) staining and **(D)** quantification of frequency of p-S6 positive cells and **(E)** p-S6 MFI of p-S6 positive cells. **(F)** CTV division peaks of SW_{HEL} B cells after *in vitro* culture for three with or without anti-CD40 and IL-21 (20 ng/ml). Statistical analysis by one-way ANOVA with Tukey's post-test (D) or t test (B, E).

Fig. 5: IL-21 modulates the BCR affinity threshold for response recruitment.
(A) Setup to study affinity-dependent effects of IL-21. **(B)** Splenic OTII Tfh count and **(C)** *Il21* locus transcription. **(D-H)** WT and *Il21r*$^{-/-}$ B cell analysis showing **(D)** representative CTV profile (data from 3-5 mice pooled mice per group), **(E)** distribution across combined CTV peaks, **(F)** ratio and **(G)** normalized cell count within each division peak (combined data from all mice) and **(H)** normalized cell counts across combined CTV peaks. B, C, E-H show data from 2 experiments with a total of 5-7 mice per group. Statistical analysis by one-way ANOVA with Tukey's post-test (B, C) or Multiple paired T tests with p values corrected for multiple comparisons using Holm-Šídák method (E, H). *$p \leq 0.05$; ** $p \leq 0.01$; *** $p \leq 0.001$.

Fig. S1: SW_{HEL} B cells characterization and flow cytometry gating strategy for Fig. 1-3.
(A, B) Lymphocytes from SW_{HEL} mouse spleen. **(C)** HEL-OVA_{pep} variant binding to SW_{HEL} B cells. **(D)** Exemplary electronic gating strategy for Fig. 1B-E to identify WT (GFP^-) and *Il21r*$^{-/-}$ (GFP^+) SW_{HEL} B cells. **(E)** Gating for Fig. 2B, 2D and 3C. SW_{HEL} B cells were identified by CTV and $HEL^{2X}OVA_{pep}$ antigen binding. eGFP was used to distinguish WT and *Il21r* $^{-/-}$ cells. Blue gates were used for analysis in Fig. 1I and red gates for Fig. 3C.

Fig. S2: Flow cytometry gating strategy for Fig. 4 and 5.
(A) Exemplary sequential electronic gating strategy as applied in Fig. 4 to identify naïve B cells following *in vitro* culture and phosphoflow staining. **(B)** Exemplary electronic gating strategy for Fig. 5B-C. OTII T cells were identified based on their co-expression of TCR Vα2 and β5 and Tfh by co-expression of PD-1 and CXCR5. **(C)** Gating strategy for Fig. 5D-H. Gates 1-4 were activated in SpectroFlo software after which CD45.2 positive cells were exported for subsequent analysis in FlowJo. For Fig. 3D, F and G, WT or *Il21r*$^{-/-}$ SW_{HEL} B

cells of the individual mice were concatenated into one file per experimental group and CTV division peaks identified using FlowJo's Proliferation tool.

Figure 1

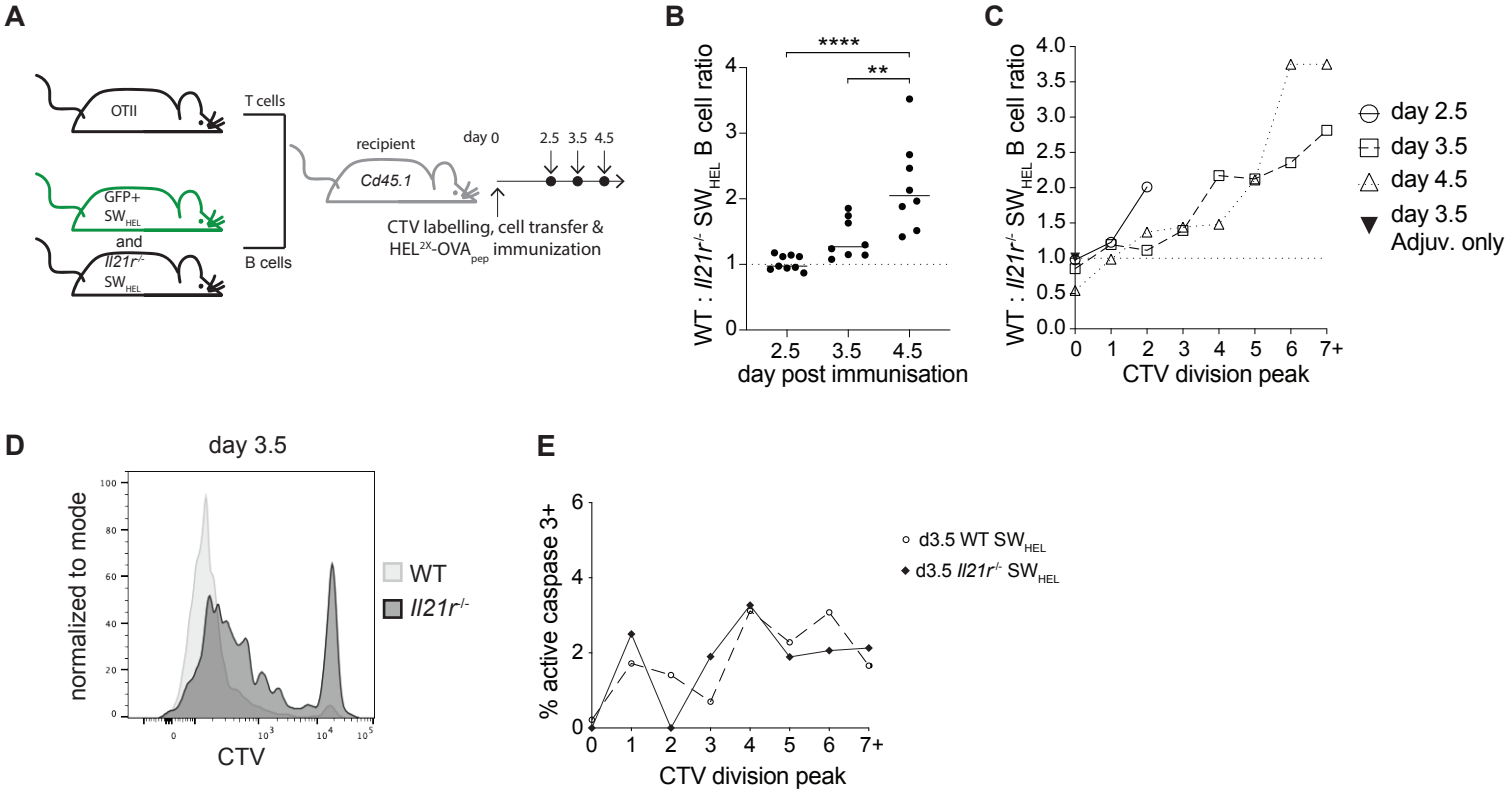

Figure 2

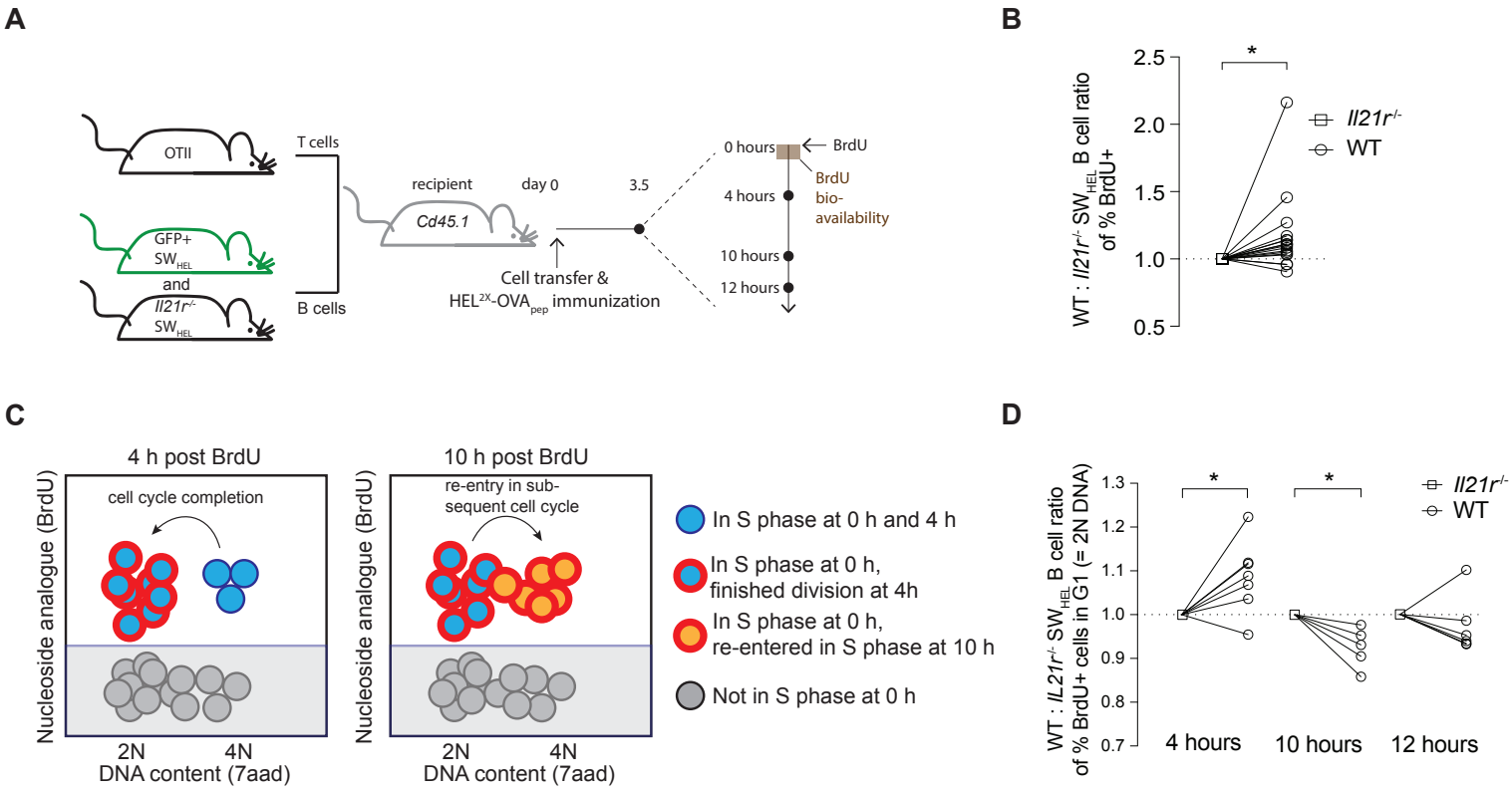

Figure 3

A

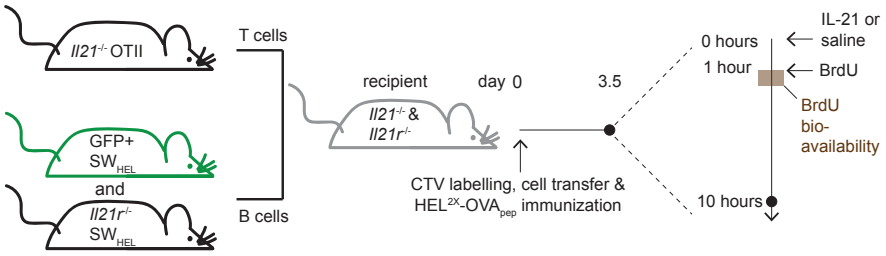

B

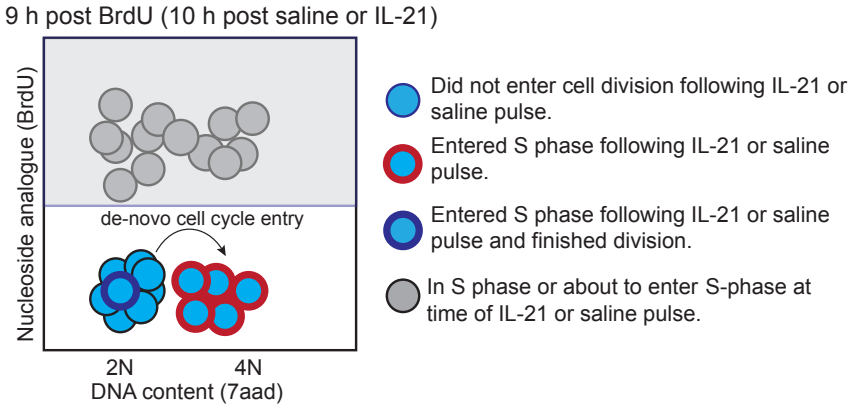

C

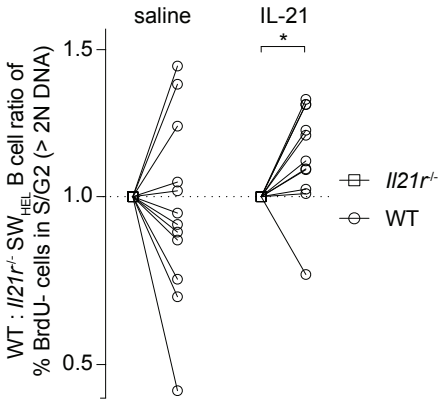

Figure 4

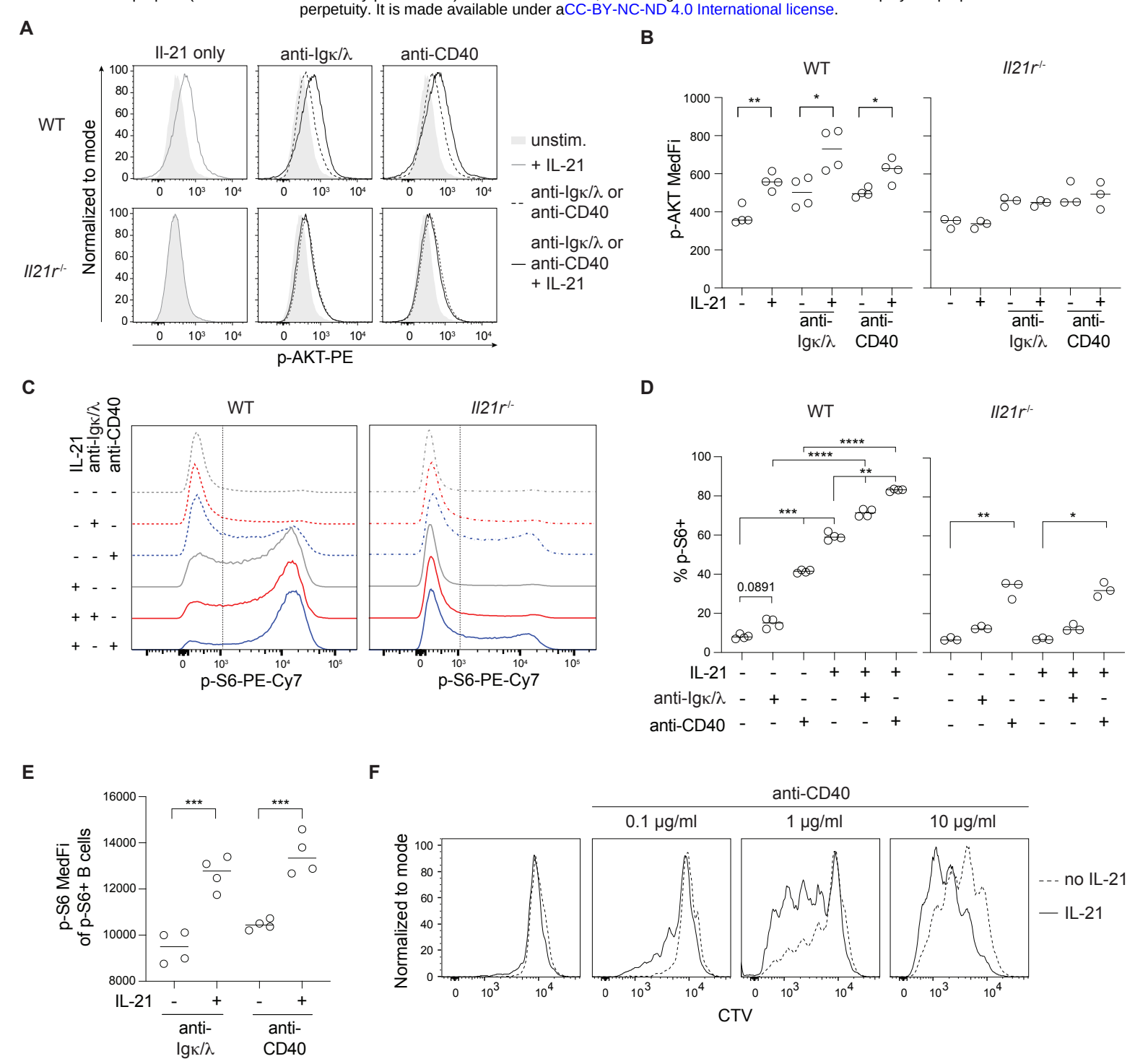

Figure 5